ANL/CHM/CP--95211

CONF-980804--

The Branching Ratio in the Thermal Decomposition of H_2CO

RECEIVED
JUL 27 1998
OSTI

by

S. S. Kumaran,* J. J. Carroll,§ and J. V. Michael
Chemistry Division, Argonne National Laboratory, Argonne, IL 60439, USA

Corresponding Author: **Dr. J. V. Michael**
D-193, Bldg. 200
Argonne National Laboratory
Argonne, IL 60439
Phone: (630) 252-3171, Fax: (630) 252-4470
E-mail: Michael@anlchm.chm.anl.gov

(27th Symp. (Int'l) on Combust., ~~October, 1997~~)

Presentation Mode: Oral Presentation
Preferred Publication: Proceedings
Category: Reaction Kinetics

	Text	Reference	Tables	Figures	Total
Count	11 pages	36 citations	2 page	2 pages	
Equiv. Words	3567	736	400	400	5103

---

*Present address: Cabot Corporation, 700 E. US Highway 36, Tuscola, IL 61953.

§Faculty Research Participant, Dept. of Educational Programs, Argonne. Permanent address: Department of Chemistry, Siena College, Loudonville, NY 12211.

This work was supported by the U. S. Department of Energy, Office of Basic Energy Sciences, Division of Chemical Sciences, under Contract No. W-31-109-Eng-38.

Abstract

The thermal decomposition of H_2CO has been investigated in reflected shock waves experiments at temperatures between 2004–2367 K. The quantitative temporal formation of H-atoms in the reactions, (1a) $H_2CO + Kr \rightarrow HCO + H + Kr$ and $HCO + Kr \rightarrow CO + H + Kr$, were measured by the atomic resonance absorption spectrometric (ARAS) technique. The product HCO-radicals instantaneously decompose giving a second H-atom. The experiments were carried out under conditions where secondary reaction perturbations were negligible. The observed H-atom profiles could be reproduced using a two step mechanism, reactions (1a) and (1b), $H_2CO + Kr \rightarrow H_2 + CO + Kr$. The resulting values for the branching ratio, $k_{1a}/(k_{1a} + k_{1b})$, range between 6.7–12.2%. The data yield second-order rate constants, $k_{1a} = 1.019 \times 10^{-9} \exp(-38706 \text{ K/T})$ and $k_{1b} = 4.658 \times 10^{-9} \exp(-32110 \text{ K/T})$ cm^3 $molecule^{-1}$ s^{-1}, respectively. The rate data and branching ratio results are compared to earlier determinations. Lastly, the data are theoretically rationalized using three theoretical formalisms. Single channel theoretical calculations are carried out with the semiempirical Troe and with the RRKM-Gorin methods, and these are compared to multichannel RRKM calculations using the *Unimol* code.

INTRODUCTION

It is well known that formaldehyde, H_2CO, is an important intermediate product in the combustion of methane and all other hydrocarbons where the CH_3-radical is a chain center [1-3]. There are nine prior studies of the thermal decomposition [4-12], and the relative importance of the two direct dissociation pathways:

$$H_2CO + Kr \rightarrow HCO + H + Kr, \qquad (1a)$$

and

$$H_2CO + Kr \rightarrow H_2 + CO + Kr, \qquad (1b)$$

is still unresolved. In experiments where $[H_2CO]_0$ is relatively high, there is no question but that it will be primarily destroyed by the atom and radical chain reaction (i. e., reaction (1a) followed by HCO decomposition to give two H-atoms which then abstract from H_2CO giving H_2 + HCO) [8,11,12]. The net process gives the same products as the direct reaction (1b). With the exception of Just [8], who reported a large contribution from reaction (1b), all prior studies were carried out with high $[H_2CO]_0$, and, therefore, little could be concluded about the importance of reaction (1b) because the results were insensitive to the reaction. However, branching between reactions (1a) and (1b) can become an important issue in high temperature systems at low $[H_2CO]_0$. The branching ratio is also interesting from a theoretical point of view. The interpretation of relative rates should be straightforward since fall-off should be minimal.

In earlier work from this laboratory on the thermal decomposition of C_2H_5I, the branching ratio to atomic *versus* molecular products was measured and discussed in terms of multichannel RRKM theoretical calculations [13]. When the threshold energy for dissociation for one channel is lower than that for a second channel, the de-population due to the low lying process should substantially enhance dissociation relative to the higher lying process if the pressure is low enough. In 1994, Just clearly described the theoretical model and implications due to these effects [14]. The H_2CO dissociation is a much better case for assessing the correctness of this expected effect because the paucity of degrees of freedom insures that the study will be at or near the low pressure limit. This should amplify the above mentioned dynamical effect [13].

EXPERIMENTAL

Apparatus:

The present experiments were performed with a shock tube, previously described [15], operating in the reflected mode. Incident shock velocities were measured with eight pressure transducers (PCB Piezotronics, Inc., Model 1132A). Final temperature and density for each experiment were determined from loading pressure and temperature and from the incident shock velocity. Corrections for non-idealities due to boundary layer formation were applied [15,16]. The photometer system was radially located 6 cm from the endplate and had an optical path length of 9.94 cm. Transmittances and the differentiated signals from the pressure transducers were recorded with a dual-channel (Nicolet 4094C) digital oscilloscope. Since the pressures of condensable gases were well below saturation, all pressure measurements with an MKS Baratron capacitance manometer in an all glass vacuum line were stable, and mixture preparation by the partial pressure method was routine. Reactant pressures were likewise measured with an MKS Baratron capacitance manometer shortly before shock firing. The time between reactant introduction into the shock tube and firing was 30 seconds.

H-atom Detection:

The ARAS technique was used to monitor $[H]_t$. As in earlier H-atom ARAS studies [17-23], the lamp was operated at 40 watts microwave power and 2 Torr of prepurified He. An atomic filter section was used to establish the fraction of non-$Ly_{\alpha\text{-}H}$ light. Enough H_2 and CH_4 impurities are present in the He to give an easily measured H-atom signal through an O_2 (1 atm of dry air) gas filter. Under these conditions, the lamp is not reversed, and a Doppler broadened calculation at an equivalent lamp temperature of 480 K with the known oscillator strength for $Ly_{\alpha\text{-}H}$ will give an exact relationship between absorbance, (ABS) = $-\ln T_r$, and [H]. This relationship is nearly linear above ~700K for $T_r = I/I_0 \geq 0.1$ [18], and we have carried out experiments to show that this procedure is accurate [23].

Kinetics Experiments:

17 kinetics experiments were carried out between 2004 and 2367 K using low initial concentrations of H_2CO. The conditions of these experiments are shown in Table 1. The loading pressure was maintained at low values (3 to 6 Torr) because background H-atoms can be and are formed from sub-ppm impurities (H_2 and CH_4) in the purest available rare gas (Kr). In the present experiments, the Kr was passed through an inert gas purification getter. Evenso, companion experiments in pure Kr, at the same total pressures and nearly the same temperatures as those in Table 1, still showed measurable H-atom formation. For the 17 experiments, we generally performed two additional pure Kr runs in order to measure the absolute $[H]_t$ from this source. Since both the impurity and H_2CO concentrations in the present work are both quite low, the formation rates from the two sources can be considered to be independent from one another. Hence, choosing the impurity experiment which most closely matches the conditions of a kinetic experiment, we subtract point-by-point the impurity experiment from the kinetics experiment. Figure 1 shows a typical $[H]_t$ against time plot where $[H]_t$ is determined from a line absorption calculation at the temperature of the experiment. This calculational procedure has already been described, and the present study exhibits ~2 times more data scatter than previous work [23] since the final H-profile is a difference between two signals with about equal signal to noise ratio. In general, the impurity ranged from 0.09-0.30 of the total $[H]_t$; i. e., 70-91% of the signal was due to H_2CO decomposition.

Gases:

High purity He (99.995%), used as the driver gas, was from Air Products and Chemicals, Inc. Scientific grade Kr (99.997%), the diluent gas in reactant mixtures, was from Spectra Gases, Inc. and was subjected to further purification by passage through a Gate Keeper inert gas purifier from Aeronex, Inc. Ultra-high purity grade He (99.999%) for the resonance lamp and high purity H_2 (99.995%) for the atomic filter were from Airco. H_2CO was prepared by heating technical grade paraformaldehyde (95%) from Aldrich Chemical Co. The collected H_2CO was outgassed and subjected to bulb-to-bulb distillation. The middle third, stored at -78 °C, was then used for mixture preparation. As an alternative H_2CO source, 99% 1,3,5 Trioxane, $(H_2CO)_3$, from Aldrich Chemical Co. was subjected to bulb-to-bulb distillation retaining the middle third. The thoroughly outgassed product had sufficient vapor pressure for accurate mixture preparation. As has been already demonstrated [11], this molecule on shock heating instantaneously gives three molecules of H_2CO.

RESULTS AND DISCUSSION

Including reaction (1b), thermal decomposition rate constants were evaluated by chemically simulating the four step chain mechanism already presented by Irdam et al. [11]. For all experiments in Table 1, the results were completely insensitive to $H + HCO \rightarrow H_2 + CO$ and $HCO + M \rightarrow H + CO + M$ because (a) [H] is so small that the former is negligible and (b) HCO decomposition is so fast that the latter can be taken to be instantaneous. We found that inclusion of $H + H_2CO \rightarrow H_2 + HCO$ with the rate constant being the theoretical value, $k = 9.53 \times 10^{-17} T^{1.9} \exp(-1380 K/T)$ cm^3 $molecule^{-1}$ s^{-1} [11], gave ≤2% perturbation in the simulated $[H]_t$. Hence, reactions (1a) (overall process being $H_2CO + Kr = 2H + CO + Kr$) and (1b) are the only reactions necessary for simulation under the present conditions. Both reactions were varied to obtain good fits to the measured profiles. An example is shown in Fig. 1 where the simulation is compared to experiment. The values thus obtained for the 17 experiments are listed in Table 1 along with the branching ratio, BR, defined as $k_{1a}/(k_{1a} + k_{1b})$. Arrhenius analyses of these data for 2004-2367 K yield:

$$k_{1a} = 1.019 \times 10^{-8} \exp(-38706 \text{ K/T}) \text{ cm}^3 \text{ molecule}^{-1} \text{ s}^{-1}, \quad (2)$$

and,

$$k_{1b} = 4.658 \times 10^{-9} \exp(-32110 \text{ K/T}) \text{ cm}^3 \text{ molecule}^{-1} \text{ s}^{-1}. \quad (3)$$

The data points are within ±21% and ±29% of eqns. (2) and (3), respectively, at the one standard deviation level.

The previous data [4-11] have already been carefully considered, and all studies have been skillfully explained by Irdam et al. [11]. These workers used a combination of earlier data and RRKM theory to suggest a rate constant for reaction (1a). They report,

$$k_{1a} = 2.693 \times 10^{12} T^{-5.54} \exp(-48666 \text{ K/T}) \text{ cm}^3 \text{ molecule}^{-1} \text{ s}^{-1}, \quad (4)$$

for the temperature range, 1600-2300 K. Eqn. (4) gives values that are lower than the present result, eqn. (2), by only 6-17% over the present temperature range. Hence, within experimental error, the present results are in excellent agreement with this earlier data. The data of Just [8] was in part used by Irdam et al. to arrive at eqn. (4). However, Just [8,24] reports for 1700-2200 K,

$$k_{1a} = 3.32 \times 10^{-8} \exp(-40124 \text{ K/T}) \text{ cm}^3 \text{ molecule}^{-1} \text{ s}^{-1}, \quad (5)$$

and for 1900-2300 K,

$$k_{1b} = 3.65 \times 10^{-9} \exp(-32350\ \mathrm{K}/T)\ \mathrm{cm^3\ molecule^{-1}\ s^{-1}}. \qquad (6)$$

For 2000-2200 K, eqn. (5) suggests values about 65% higher than eqn. (2) whereas eqn. (6) suggests values about 70% of eqn. (3). Irdam et al. also comment on reaction (1b) suggesting that the branching ratio can be no less than 0.25-0.33 for 2000-3000 K. The main conclusions from the present work and the study by Just is that the branching ratio is substantially lower, being 0.07-0.21. In the experiments by Eiteener et al. [12], inclusion of reaction (1b) was unnecessary due primarily to the relatively high levels of $[H_2CO]_0$ used; i. e., the chain reaction completely dominates the destruction. The fitted value, using the GRI mechanism 2.11 [2], implies values about four times larger than eqn. (2).

In order to explore the differences between the present work and the above mentioned studies, we have carried out our own theoretical calculations using recent accurately determined values for threshold energies for both reaction (1a), E_{01a} = 86.705 kcal mole^{-1} [25], and reaction (1b), E_{01b} = 79.200 kcal mole^{-1} [26]. The properties of the asymmetric transition state for reaction (1b) have additionally been determined using *ab initio* electronic structure calculations [26]. All quantities necessary for the calculations are summarized in Table 2.

Following recent work from this laboratory [13], second-order dissociation rate constants for both channels have been theoretically calculated with two single channel models; i. e., method (a), semiempirical Troe [30] and method (b), RRKM. In addition, we have also carried out multichannel *Unimol* RRKM calculations (i. e., method (c)) [13,31]. All three methods include appropriate weak collision corrections through the efficiency factor, β_c, set by the average energy transfer parameter, $\langle \Delta E \rangle_{down}$ or, alternatively, $-\langle \Delta E \rangle_{all}$. Method (a) [30] utilizes the Whitten-Rabinovitch formula for calculating the density of states whereas both methods (b) and (c) use direct count algorithms. Standard fall-off calculations of the unimolecular rate constants result from all three methods. The accounting of weak collisional effects are similar for both single channel methods; however, in the *Unimol* code, a full master equation calculation evaluates the effects of de-population at low pressures on the higher lying channel due to the presence of the lower lying channel. The single channel models (a) and (b) consider both channels to be completely independent from one another.

Using $E_{01a} = 86.705$ kcal mole^{-1} with the semiempirical Troe method (a), the present data require $-\langle \Delta E \rangle_{all}^{1a} = 119$ cm^{-1} between 2000-2400 K. High pressure rate constant evaluation for the back reaction using the previously described Lennard-Jones model [32] gives a nearly T-independent value, $k_{-1a} = (3.90 \pm 0.12) \times 10^{-10}$ cm^3 molecule^{-1} s^{-1} (2000-2400 K). The equilibrium constant for reaction (1a) can be calculated from the molecular quantities in Table 2 yielding:

$$K_{eq}^{1a} = 2.985 \times 10^{25} \exp(-43765 \text{ K/T}) \text{ molecules cm}^{-3}, \qquad (7)$$

thereby implying a value for the high pressure limit for reaction (1a) (within ±0.1%) of:

$$k_{\infty}^{1a} = 1.618 \times 10^{16} \exp(-44486 \text{ K/T}) \text{ s}^{-1}. \qquad (8)$$

The limiting low pressure value, $k_0^{1a} = \beta_c^{1a} k_{0sc}^{1a}$, to within 0.01% is:

$$k_0^{1a} = 6.906 \times 10^{9}\, \text{T}^{-4.746} \exp(-48412 \text{ K/T}) \text{ cm}^3 \text{ molecule}^{-1} \text{ s}^{-1}. \qquad (9)$$

Eqns. (8) and (9) are included in Table 2. Comparison of the experimental result, eqn. (2), with eqn. (9) shows only ~7-12% fall-off over the present T- and P-ranges. Hence, this reaction is near the low pressure limit.

For reaction (1b), similar semiempirical Troe calculations with method (a) have been carried out using E_{01b} = 79.200 kcal mole^{-1}. In order to fit the present data between 2000-2400 K, $-\langle \Delta E \rangle^{1b}_{all}$ = 390 cm^{-1} is required. In this case, the high pressure rate constant can be directly evaluated from the transition state properties shown in Table 2 (including Wigner tunneling) yielding to within ±0.1%:

$$k^{1b}_{\infty} = 3.828 \text{ x } 10^{14} \exp(-41541 \text{ K/T}) \text{ s}^{-1}. \tag{10}$$

The limiting low pressure value, $k^{1b}_{0} = \beta^{1b}_{c} k^{1b}_{0sc}$, to within 0.2% is:

$$k^{1b}_{0} = 2.148 \text{ x } 10^{10} \text{ T}^{-4.799} \exp(-44910 \text{ K/T}) \text{ cm}^{3} \text{ molecule}^{-1} \text{ s}^{-1}. \tag{11}$$

Eqns. (10) and (11) are also included in Table 2. For 2000-2400 K, the present experimental results for reaction (1b) are summarized by eqn. (3), and these results can be compared to the low pressure limit, eqn. (11). Eqn. (3) gives values ~9-25% lower than eqn. (11) showing that the reaction is still near to the low pressure limit. However, this reaction falls off faster over the present T- and P-ranges than reaction (1a). Figure 2 shows an Arrhenius plot of the present rate constants (Table 1) for both channels in comparison to the theoretical predictions from method (a) using the parameters listed in Table 2.

The second method (b) is a full RRKM calculation [32]. In this case, channel (1a) is evaluated by using a restricted rotor Gorin model [33,34] where the bond-fission transition state is considered, as described earlier, to be a loosely bound product-like moiety [32]. Two external rotations with the largest moments are treated as adiabatic and have a size that is temperature dependent according to the usual Gorin prescription. The last external rotation and the two bending degrees of freedom are nominally treated as free internal rotors with moments of inertia fixed at that for the isolated HCO product. In a correction to the looseness of three internal rotations, a factor, (1 - η), multiplies the free rotor partition function to effectively determine the high-pressure A-factor. The hindrance parameter, η, used here assumes 95% hindrance. These properties of the transition state completely determine A_{∞}^{1a}. RRKM calculations were also carried out for the second channel (1b) with the transition state properties for the elimination channel shown in Table 2. The results from both calculations are summarized in the table where it can be seen that the results for the A_{∞}'s from methods (a) and (b) are almost identical for (1a) and are identical for (1b). The values from both methods for the k_0's are also summarized in Table 2. Again, the comparison between methods is excellent. The energy transfer values necessary to explain the data with the RRKM method (b) requires $-\langle \Delta E \rangle_{all}^{1a} = 31$ cm^{-1} and $-\langle \Delta E \rangle_{all}^{1b} = 231$ cm^{-1}, and these would seem to disagree with the method (a) semiempirical Troe values mentioned above. The discrepancy for (1a) can be explicitly traced to the value for $I^{\ddagger}/I = 2.15\ (E_0/RT)^{0.33}$, from the Gorin model that is used in the evaluation of F_{rot}, to be contrasted to that used in the Lennard-Jones model; i. e., the ratio of the Lennard-Jones diatomic moment divided by the largest moment in the H_2CO molecule. Hence, k_{0sc}^{1a} from the Gorin prescription is ~6 times bigger than that from the semiempirical model. We also note that the direct count state densities are ~30% smaller than the Whitten-Rabinovitch evaluations for both channels, and this explains the remaining discrepancy between methods (a) and (b). Since all energy transfer values are adjusted to make theory coincident with the data, the final comparison of results is excellent for both channels from methods (a) and (b), using the parameters listed in Table 2, and the RRKM method (b) values are then nearly superimposable with the theoretical lines from method (a) shown in Fig. 2.

With either method (a) or (b), the calculations of the two rate constants for the present conditions agree quite closely with the experimental results summarized by eqns. (2) and (3) and shown in Fig. 2. Hence, theory can rationalize the observed branching ratio within experimental error. We note however that the low values found here ($0.07 \leq BR \leq 0.12$) are caused by the low total pressures used in the present experiments.

Comparison of the limiting high pressure rate constants (e. g., for method (a), eqns. (8) and (10)) shows that as pressure increases, reaction (1a) will eventually dominate giving BR = (0.92 ± 0.01) for 2000-2400 K. Hence, any value between these limits is possible depending on pressure. The results of Just, eqns. (5) and (6), were obtained at ~10 times greater total density than the present, and they imply slightly higher BR values. However, using the present theory, greater density cannot reconcile the differences. For example, using method (a), the broadening factors are functions of the reduced pressure, $P_r \equiv \beta_c k_{0sc}[M]/k_\infty$. The minimum values of broadening factors for the two reactions occur at Pr = 1 implying minima for reaction (1a) and (1b) at $[M] \cong 1 \times 10^{23}$ and 1×10^{21} molecules cm^{-3}, respectively; i. e., the effects of pressure fall-off and substantial variation in BR would only be observable at pressures >100-200 atm. With the present single channel semiempirical method, the energy transfer parameters would have to be varied to explain the BR results of Just.

In an attempt to understand the effects of population depletion on channel (1a) due to the presence of (1b) and to perhaps explain the slight differences between the present results and those of Just, we have also carried out multichannel RRKM calculations using the *Unimol* code (method (c)). Again, the molecular parameters used are the same as in methods (a) and (b); i. e., those from Table 2. The energy transfer parameter necessary to explain the absolute rate constant values for (1b) is between those found using methods (a) and (b); i. e., $-\langle \Delta E \rangle_{all}^{1b} = 333$ cm^{-1}. However, for reaction (1a) with this same $-\langle \Delta E \rangle_{all}$ value, the predicted rate constants for H-atom formation are only 5.8–8.2% of the experimental values (eqn. 2)), indicating that the *Unimol* model completely overestimates the population depletion effect. Theory would suggest BR values ranging from 6.6-7.8 x 10^{-3} over the present temperature range. The values for limiting high pressure rate constants, listed in Table 2, are in adequate agreement with those from methods (a) and (b), and the limiting low pressure rate constant for reaction (1b) is also close to those from these earlier methods. The *Unimol* value for the (1a) low pressure limit reflects the population depletion effects due to the lower lying reaction (1b).

The H_2CO decomposition has properties that make it one of the best candidates for detailed theoretical study. Threshold energies are known from spectroscopic studies with high accuracy [25,26]. The state densities are so low that the reaction is always near to the low pressure limit, and therefore, the collisional efficiency factors can be obtained with high accuracy. Even though the single channel models (a) and (b) can rationalize the present data, the values for the energy transfer parameters are puzzling. One expects increasing values with increasing threshold energies; however, the value for the higher is substantially smaller than that for the lower channel. Also, the multichannel calculation simply fails to appropriately explain the BR values measured here or in the work of Just. Hence, there is a serious breakdown of theory for H_2CO. We can only speculate as to the cause for this breakdown. The experimental state count at the threshold energy in D_2CO is (437 ± 112) states cm^{-1} indicating about an order of magnitude discrepancy between the harmonic direct count and the experimental direct count [26]. The same relationship is expected for H_2CO. A similar discrepancy has also been noted in C_2H_2 [35]. Clearly, rotational states are contributing to the total state density at threshold energies, and this is not appropriately taken into account with current unimolecular theories. The question as to what rotations are adiabatic or active in both transition states and active molecules has always been ambiguous. This question has recently been raised again by Hase and coworkers [36] in a discussion of the $Cl + C_2H_2$ reaction. If the theory were somehow corrected for these effects, then the derived energy transfer parameters would change substantially, perhaps indicating more fall-off behavior with pressure. Then the *Unimol* code might give sensible predictions, and the slightly higher branching ratios from Just might then be rationalized.

Acknowledgment: The authors thank Dr. A. F. Wagner for useful discussions. This work was supported by the U. S. Department of Energy, Office of Basic Energy Sciences, Division of Chemical Sciences, under Contract No. W-31-109-Eng-38.

---

1 Warnatz, J., in *Combustion Chemistry*, Gardiner, W. C. Jr., Ed., Springer, Heidelberg, 1984, p. 197.

2 Bowman, C. T., Hanson, R. K., Davidson, D. F., Gardiner, W. C. Jr., Lissianski, V., Smith, G. P., Golden, D. M., Frenklach M. and Goldenberg, M., *GRI Mechanism 2.11*, http://www.me.berkeley.edu/gri_mech/

3 Pilling, M. J., Turanyi, T., Hughes, K. J. and Clague, A. R., *The Leeds Methane Mechanism 1.3,* http://www.chem.leeds.ac.uk/Combustion/Combustion.html

4 Gay, I. D., Glass, G. P., Kistiakowsky, G. B. and Niki, H., *J. Chem. Phys.* 43:4017-4022 (1965)

5 Schecker, H. and Jost, W., *Ber. Bunsenges. Phys. Chem.* 73:521-526 (1969)

6 Dean, A. M., Craig, B. L., Johnson, R. L., Schultz, M. C. and Wang, E. E., *Seventeenth Symposium (International) on Combustion*, The Combustion Institute, Pittsburgh, 1979, pp. 577–584.

7 Dean, A. M., Johnson, R. L. and Steiner, D. C., *Combust. Flame* 37:41-xx (1980)

8 Just, Th., in *Shock Waves in Chemistry*, Lifshitz, A., Ed., Dekker, New York, 1981, pp. 279-318.

9 Saito, K., Kakumoto, T., Nakanishi, Y. and Imamura, A., J. Phys. Chem. 89:3109-3113 (1985)

10 Buxton, J. P. and Simpson, C. J. S. M., *Chem. Phys. Lett.* 129:577-582 (1986)

11 Irdam, E. A., Kiefer, J. H., Harding, L. B. and Wagner, A. F., *Int. J. Chem. Kinet.* 25:285-303 (1993)

12 Eiteneer, B., Yu, C.-L., Goldenberg, M. and Frenklach, M., *Western States Meeting of the Combustion Institute*, U. of Southern California, Los Angeles, October, 1996.

13 Kumaran, S. S., Su, M.-C., Lim, K. P. and Michael, J. V., *Twenty-Sixth Symposium (International) on Combustion*, The Combustion Institute, Pittsburgh, 1996, pp. 605-611.

14 Just, Th., *Twenty-Fifth Symposium (International) on Combustion*, The Combustion Institute, Pittsburgh, 1994, pp. 687-703.

15 Michael, J. V., *Prog. Energy Combust. Sci.* 18:327–347 (1992), and references cited therein.

16 Michael, J. V., and Sutherland, J. W., *Int. J. Chem. Kinet.* 18:409–436 (1986)

17 Lynch, K. P., Schwab, T. C. and Michael, J. V., *Int. J. Chem. Kinet.* 8:651–671 (1976)

18 Maki, R. G., Michael, J. V. and Sutherland, J. W., *J. Phys. Chem.* 89:4815–4821 (1985)

19 Michael, J. V. and Wagner, A. F., *J. Phys. Chem.* 94:2453–2464 (1990)

20 Michael, J. V., *J. Chem. Phys.* 92:3394–3402 (1990)

21 Shin , K. S. and Michael, J. V., *J. Phys. Chem.* 95:5864–5869 (1991)

22 Shin, K. S. and Michael, J. V., *J. Chem. Phys.* 95:262–73 (1991)

23 Lim, K. P. and Michael, J. V., *Twenty-Fifth Symposium (International) on Combustion*, The Combustion Institute, Pittsburgh, 1994, pp. 713-719.

24 Just, Th., private communication, October, 1997.

25 Terentis, A. C. and Kable, S. H., *Chem. Phys. Lett.* 258:626-632 (1996)

26 Polik, W. F., Guyer, D. R. and Moore, C. B., *J. Chem. Phys.* 92:3453-3470 (1990)

27 Yamada, K., Nakagawa, T., Kuchitsu, K. and Morino, Y., *J. Molec. Spectros.* 38:70-83 (1971)

28 Werner, H.-J., Bauer, C., Rosmus, P., Keller, H.-M., Stumpf, M. and Schinke, R., *J. Chem. Phys.* 102:3593-3611 (1995)

29 Blake, G. A., Sastry, K. V. L. N. and DeLucia, F. C., J. Chem. Phys. 80:95-101 (1984)

30 Troe, J., *J. Chem. Phys.* 66: 4745-4757 (1977); *ibid.* 66: 4758-4775 (1977); Troe, J., *J. Phys. Chem.* 83: 114-126 (1979); Troe, J., *Ber. Bunsenges. Phys. Chem.* 87: 161-169 (1983); Gilbert, R. G., Luther, K., and Troe, J., *Ber. Bunsenges. Phys. Chem.* 87: 169-177 (1983)

31 Gilbert, R. G., Smith, S. C., and Jordan, M. J. T., *Program package UNIMOL program suite (1993)*, School of Chemistry, Sydney University, NSW 2006, Australia, Gilbert_R@summer.chem.su.oz.au

32 Kumaran, S. S., Su, M,-C., Lim, K. P., Michael, J. V. and Wagner, A. F., *J. Phys. Chem.* 100:7533-7540 (1996)

33 (a) Benson, S. W. and Golden, D. M. in *Physical Chemistry, An Advanced Treatise, Vol.* VII, Eyring, H., Henderson, D. and Jost, W., Eds., Academic Press, New York, 1975. (b) Smith, G. P. and Golden, D. M., *Int. J. Chem. Kinet.* 10:489-501 (1978)

34 Smith, G. P., Manion, J. A., Rossi, M. J., Rodgers, A. S. and Golden, D. M., *Int. J. Chem. Kinet.* 26:211-217 (1994)

35 Abramson, E., Field, R. W., Imre, D., Innes, K. K. and Kinsey, J. L., *J. Chem. Phys.* 83:453–465 (1985)

36 Zhu, L., Chen, W., Hase, W. L. and Kaiser, E. W., *J. Phys. Chem.* 97:311–322 (1993)

Table 1: Rate Data for the H_2CO Thermal Decomposition

P_1 / Torr	[a]M_s	[b]ρ_5 / (10^{18} cm^{-3})	[b]T_5 / K	[c]k_{1a}	[c]k_{1b}	[d]BR
$X_{H_2CO} = 7.208 \times 10^{-6}$						
5.96	2.893	1.294	2057	5.18(-17)	3.88(-16)	0.118
5.93	3.064	1.349	2284	3.11(-16)	2.43(-15)	0.113
5.94	3.013	1.334	2212	1.95(-16)	1.62(-15)	0.107
5.96	2.943	1.316	2117	9.88(-17)	8.05(-16)	0.109
4.51	2.947	0.997	2122	1.10(-16)	1.26(-15)	0.080
4.56	3.034	1.026	2250	3.60(-16)	3.32(-15)	0.098
4.51	3.102	1.035	2337	6.77(-16)	5.04(-15)	0.118
4.52	2.857	0.975	2004	6.15(-17)	8.61(-16)	0.067
3.06	2.934	0.672	2112	1.12(-16)	1.43(-15)	0.073
3.10	2.969	0.689	2153	1.60(-16)	1.92(-15)	0.077
3.08	3.004	0.690	2200	2.46(-16)	2.61(-15)	0.086
3.07	2.962	0.681	2143	1.39(-16)	1.26(-15)	0.099
$X_{(H_2CO)_3} = 2.311 \times 10^{-6}$						
3.04	3.002	0.681	2198	2.13(-16)	2.30(-15)	0.085
3.05	2.991	0.682	2183	2.54(-16)	2.22(-15)	0.103
3.08	2.906	0.673	2068	8.17(-17)	9.56(-16)	0.079
3.00	3.071	0.683	2293	6.29(-16)	4.78(-15)	0.116
3.04	3.123	0.701	2367	9.70(-16)	6.99(-15)	0.122

---

[a] The error in measuring the Mach number, M_S, is typically 0.5-1.0 % at the one standard deviation level. [b] Quantities with the subscript 5 refer to the thermodynamic state of the gas in the reflected shock region. [c] The rate constants (parentheses denote the power of ten), derived as described in the text, are in units, cm^3 $molecule^{-1}$ s^{-1}. [d] BR is the branching ratio, $k_{1a} / (k_{1a} + k_{1b})$.

Table 2: Theoretical Calculations for: H_2CO (+ M) → Prods.

Species	Frequencies (cm^{-1})	Moments of Inertia/10^{-40} gm cm^2	Source
H_2CO	2997, 2978, 1778, 1529, 1299, 1191	2.92, 21.48, 24.42	ref. 26,27
HCO	2434, 1868, 1081	1.15, 18.74, 20.02	ref. 28,29
$CO\text{-}H_2^{\ddagger}$	3132, 1855, 1351, 856, 805, 1941i	3.27, 23.33, 26.91	ref. 26

Theoretical Fits:	E_0/kcal $mole^{-1}$	$-\langle \Delta E \rangle_{all}/cm^{-1}$
(1) C-H fission		
(a) Troe semiempirical	86.705	119
(b) RRKM-Gorin	86.705	31
(c) *Unimol*	86.705	333
(2) H_2 elimination		
(a) Troe semiempirical	79.200	390
(b) RRKM	79.200	231
(c) *Unimol*	79.200	333

Theoretical Results (2000-2400 K):

	$^a\log\left(\frac{A_0}{cm^3 molecule^{-1} s^{-1}}\right)$	n_0	T_0	$\log\left(\frac{A_\infty}{s^{-1}}\right)$	T_∞
(1a) C-H fission					
(a) Troe semiempirical	9.8392	-4.746	48412	16.209	44486
(b) RRKM-Gorin	−8.5968	0	35412	16.085	44146
(c) *Unimol*	−9.9777[b]	0	34472	16.145	44560
(1b) H_2 elimination					
(a) Troe semiempirical	10.3320	-4.799	44910	14.583	41541
(b) RRKM	−8.0228	0	33343	14.583	41541
(c) *Unimol*	−8.3120	0	31962	14.580	41723

---

[a] $k_i = A_i T^{n_0} \exp(-T_i/T)$ theoretical fits for limiting low- and high-pressure rate constants.

[b] Using the *Unimol* code, the value for k_{0sc}^{1a} in $k_0^{1a} = \beta_c^{1a} k_{0sc}^{1a}$ takes into account the effects of population depletion due to reaction (1b)

Figures

Fig. 1. A typical experimental record showing increasing $[H]_t$ produced from reaction (1a). The experimental conditions are: $T_5 = 2337$ K, $P_5 = 250$ Torr, $\rho_5 = 1.035 \times 10^{18}$ cm^{-3}, and $X_{H_2CO} = 7.208 \times 10^{-6}$. The solid line is the simulated $[H]_t$ from parametric variations of rate constants for reactions (1a) and (1b). The values are listed in Table 1: $k_{1a} = 6.77(-16)$ and 5.04(-15) both in cm^3 molecule^{-1} s^{-1}, yielding a branching ratio of 0.118.

Fig. 2. Arrhenius plot of the experimental data (Table 1) for reactions (1a) (bottom) and (1b) (top). The lines shown are theoretically calculated using method (a) with the parameters given in Table 2.

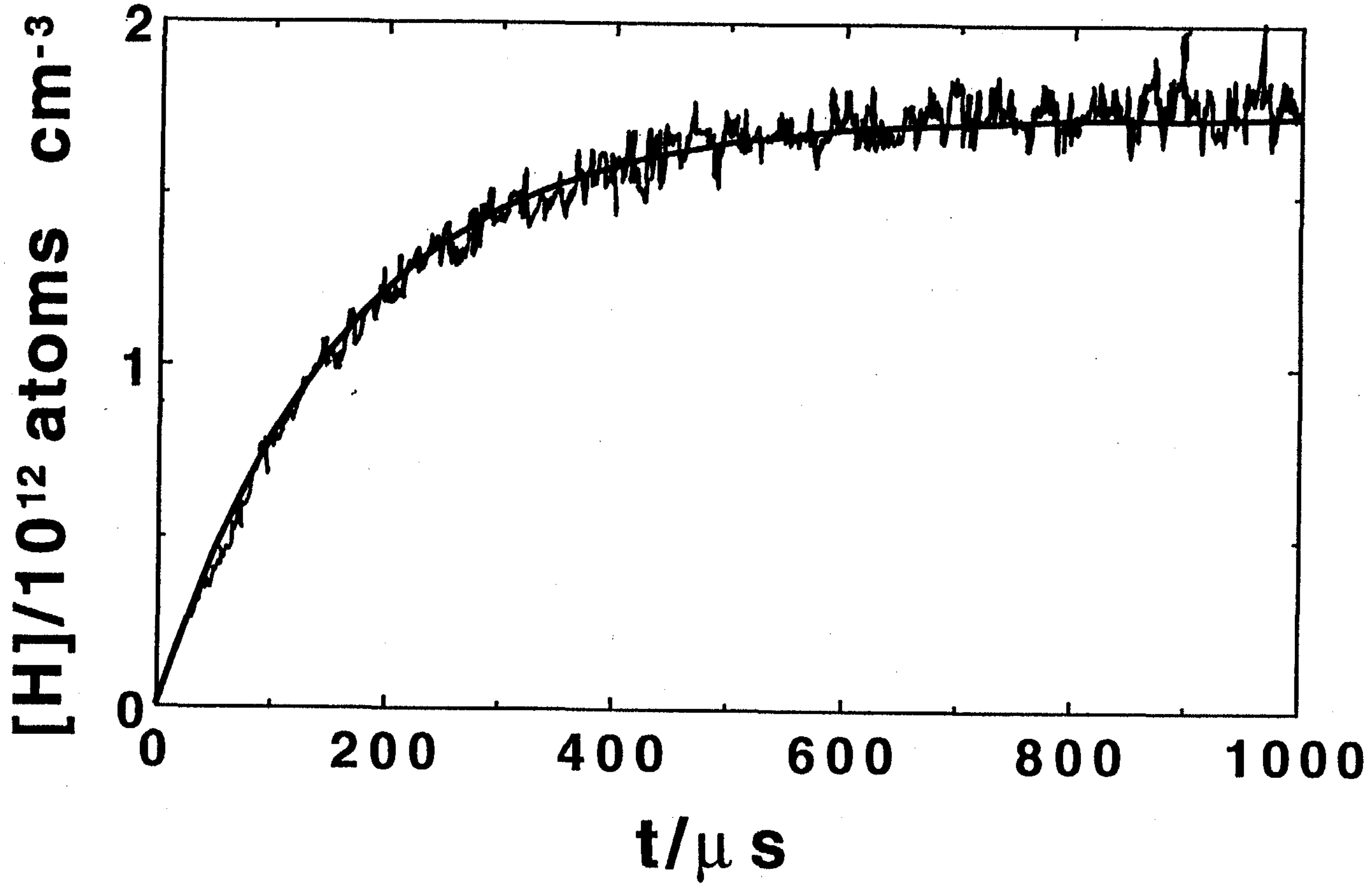
[H]/10^12 atoms cm^-3
0
1
2
0
200
400
600
800
1000
t/μ s

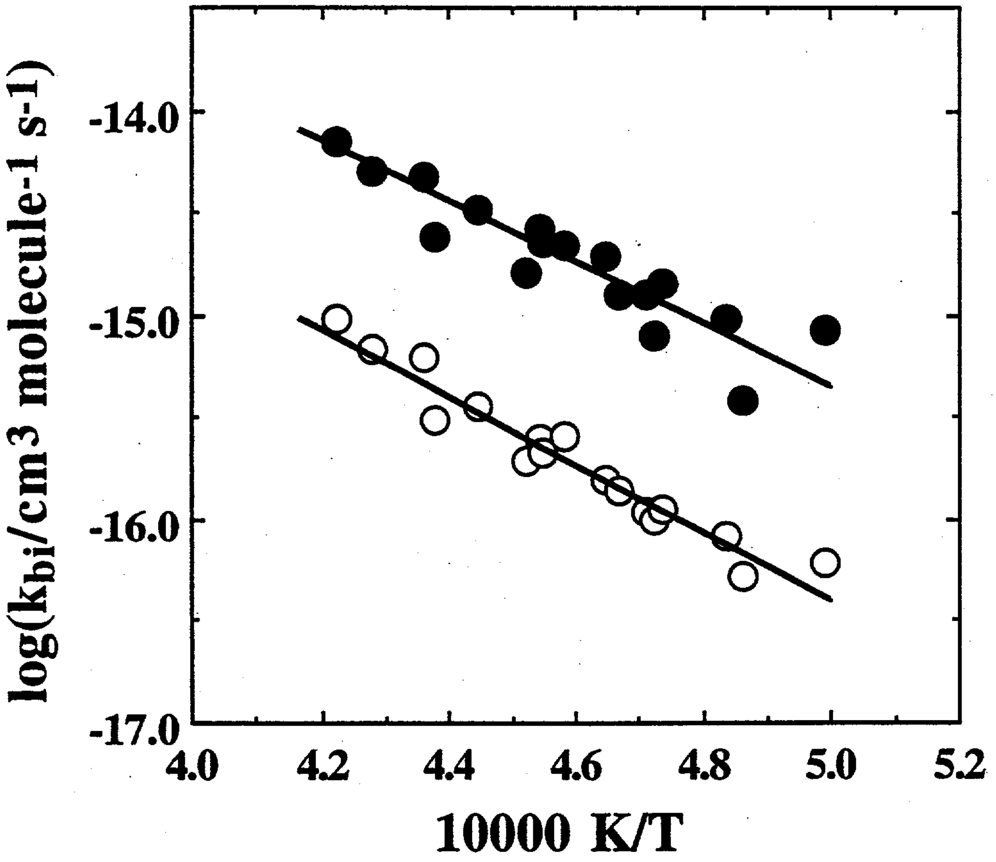
log(k_bi/cm3 molecule-1 s-1)
-14.0
-15.0
-16.0
-17.0
4.0
4.2
4.4
4.6
4.8
5.0
5.2
10000 K/T